Available online at www.sciencedirect.com
SCIENCE DIRECT®
Surface Science 595 (2005) 40–48
SURFACE SCIENCE
www.elsevier.com/locate/susc

Investigation of the geometric and electronic structures of $ErSi_{(2-x)}$ with the density functional theory and comparison with STM images

E. Duverger *, F. Palmino, E. Ehret, J.-C. Labrune

Universit de Franche Comt, Institut FEMTO-ST Dpt CREST, CNRS UMR 6174, 4 place Tharradin, BP 71427, 25211 Montbeliard Cedex, France

Received 14 March 2005; accepted for publication 27 July 2005
Available online 18 August 2005

Abstract

Study of $ErSi_{(2-x)}$ surfaces system is submitted at one controversy in reason of the STM images bias voltage dependence. In this article, we have investigated by means of calculations issued of the density functional theory (DFT), atomic surface density for 2D and 3D epitaxial erbium silicide on Si(1 1 1). DOS (density of state) in front of the surface, calculated with Wien2k, permits to simulate scanning tunneling microscopy (STM) images in function of the bias voltage and to discriminate the different surface arrangements. The calculations confirm the model of structure accepted and give some new elements in order to close the controversy on the question.

Keywords: Erbium; Silicon surface; STM; Wien2k simulation; Interface; Density functional theory

1. Introduction

Thin films epitaxy of metal silicide on silicon substrates have been subject to numerous investigations in order to clarify the mechanisms that control the interface reconstruction and the surface formation [1–3]. Some rare earth (RE) silicides have attracted a considerable attention as model candidates for heteroepitaxial growth on Si(1 1 1) due to their low lattice mismatch with Si(1 1 1), their formation at low temperature and their low Schottky-barrier on n-type silicon [4–9]. Their unusual properties make them attractive for potential electronic applications [10–16]. Among the RE silicides, $ErSi_{(2-x)}$ have been intensively studied by different techniques sensitive to the surface. The $ErSi_2$ disilicide is formed for a submonolayer range

* Corresponding author. Tel.: +33 3 81 99 46 88; fax: +33 3 81 99 46 10.
E-mail address: eric.duverger@pu-pm.univ-fcomte.fr (E. Duverger).

0039-6028/$ - see front matter © 2005 Elsevier B.V. All rights reserved.
doi:10.1016/j.susc.2005.07.036

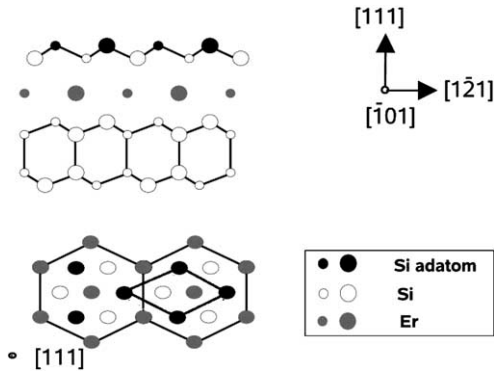

Fig. 1. $ErSi_2$ structure. In the side view, the smaller circles indicate atoms lying below cut plane. The top view (substrate deleted) represents the p(1 × 1) structure unit cell limited by large black lines.

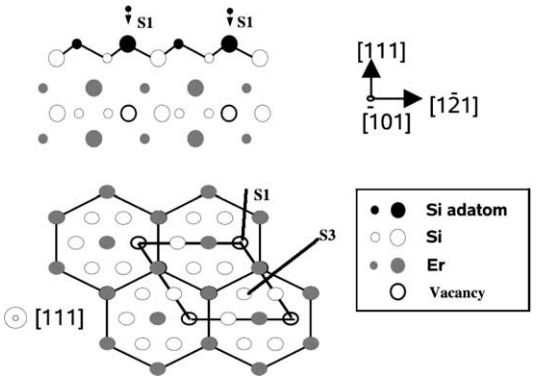

Fig. 2. $ErSi_{1.7}$ structure. In the side view, the smaller circles indicate atoms lying below cut plane. The top view (substrate deleted) represents the $(\sqrt{3} \times \sqrt{3})R30^\circ$ structure unit cell generated by the vacancies.

Er deposition on the Si(1 1 1) substrate. Its atomic arrangement can be viewed as a hexagonal erbium plane sandwiched between the Si substrate and a buckled Si top layer that closely resembles to the termination of the unreconstructed Si(1 1 1) surface. This top layer is rotated by 180° with the substrate bilayers (Fig. 1). This structure exhibits a p(1 × 1) reconstruction.

At higher erbium coverage, the 3D $ErSi_{1.7}$ silicide is formed. It crystallizes in a hexagonal phase of AlB_2 type, formed by an alternative stacking of hexagonal erbium and graphite-like Si plane along the [1 1 1] direction [3,9,17,18]. The $ErSi_{1.7}$ silicide is considered as a 2 ML $ErSi_{1.7}$ slab that involves a single defected Si plane sandwiched by two hexagonal erbium planes [6,19,20]. The outermost Si atoms called S1 are located right above the Si vacancies (Fig. 2). The existence of these vacancies modifies the number of unpaired electrons or dangling bonds. As a result, peculiar, but regular atomic arrangements occur between the atomic layers and the surface in order to stabilize the structure [3,5,9,18].

The surface periodicity observed by scanning tunneling microscopy (STM) is bias voltage dependent and both $(\sqrt{3} \times \sqrt{3})R30^\circ$ and p(1 × 1) reconstructions can be observed [18,21]. Relations between the bias dependence modulations of STM images and local density of states (LDOS) of these structures are not well established. To close the controversy, surface superstructures are simulated to obtain the theoretical local density of states (LDOS) above the surface. Via the Tersoff–Hamann formulation, we correlate theoretical results to experimental STM data and give a justification of the modulation observed in function of tip-sample bias voltage.

2. Theoretical method

Self-consistent calculations of total energy and electronic structure in polarized spin were carried out using the Wien2k code [22]. They are based on the scalar relativistic full-potential (FP) augmented plane wave plus local orbitals method (APW + lo). This is a very accurate and efficient scheme to solve the Kohn–Sham equations of density functional theory (DFT). In this case, the exchange and correlation effects are treated for example, by the generalized gradient approximation (GGA) that often leads to better energetic and equilibrium structure than the local density approximation (LDA). Electronic density is obtained by summing over all occupied Kohn–Sham orbitals and plays a key role in this formalism. A muffin tin radius of 2.0 and 2.35 a.u. has been used, respectively for Si and Er. The energy cut-off was set to 80 eV. The required precision in total energy was achieved by using a large plane wave (PW) cut-off. In the linear APW (LAPW) method,

the relevant convergence parameter is RK_{max}. It is defined by the product of the smallest atomic sphere radius times the largest reciprocal lattice vector of the PW basis. We have used $RK_{max} = 6.5$ for the structure. The k mesh was generated in the irreducible wedge of the Brillouin zone limited to 60 points. The $ErSi_2$ and $ErSi_{1.7}$ surfaces were modeled as a periodic slabs supercell with a vacuum region of 25 Bohrs. Constant-current STM topography was simulated by calculating local density of states in the vacuum in function of energy. We have evaluated isosurfaces of constant density and determined the corrugation of these isosurfaces following the Tersoff–Hamann scheme. We have combined this theory for tunneling between a real surface and a model probe tip with our ab initio calculations. When the tip is replaced by a point probe, the tip wave functions are completely localized. The tunneling current becomes proportional to the density of state in the cases of small voltage and small temperature; the tunneling current matrix becomes an identity matrix (case of STM images in atomic resolution) [23]. Typically, the isosurfaces are determined at an average distance of the surface. In our case, we have taken a distance of 2.5 Å, from the core of the outermost atoms.

3. Experimental procedure

Experiments were performed in a two-chamber ultra-high vacuum system (under a pressure below 3×10^{-10} mbar) equipped with an Omicron STM and LEED/AES facilities. The Si(1 1 1) substrate (1–3 Ω cm resistivity) is carefully degassed and cleaned in situ by series of rapid heating up to 1200 °C under a pressure lower than 5×10^{-10} mbar, and subsequently slowly cooled down in order to obtain the (7×7) reconstruction. Er deposition was performed using an e-beam evaporator onto the Si(1 1 1) substrates at about 0.1 ML min^{-1}. One monolayer is referred to the Si(1 1 1) ideal surface atomic density (7.8×10^{-14} atom cm^{-2}). Er was deposited onto the substrate at room temperature (RT) and subsequently annealed at 500 °C. Both LEED and STM observations were made at room temperature, and the STM images were acquired in the constant-current mode with bias voltage applied to the sample.

4. Results and discussion

4.1. The $ErSi_2$ surface

The 2D Er silicide surface reveals a sixfold hexagonal rotational symmetry and the LEED pattern a $p(1 \times 1)$ reconstruction. High-resolution STM images can be achieved and relevant filled state of the 2D silicide is displayed (Fig. 3). Periodicity measured in plane corresponds to the $p(1 \times 1)$ unit cell of hexagonal Si(1 1 1) or epitaxial ErSi(0 0 0 1) atomic planes.

All protrusions are imaged with an equal intensity. All the sites are undeniably structurally equivalent. No bias voltage dependence is observed in the few tens of mV range where the atomic resolution can be obtained. In order to interpret high-resolution STM images, we have used the Wien2k code. This code permits to discriminate contribution due to each atoms and the importance of electronic structure effects. We obtain data about density of state near the Fermi level that contribute

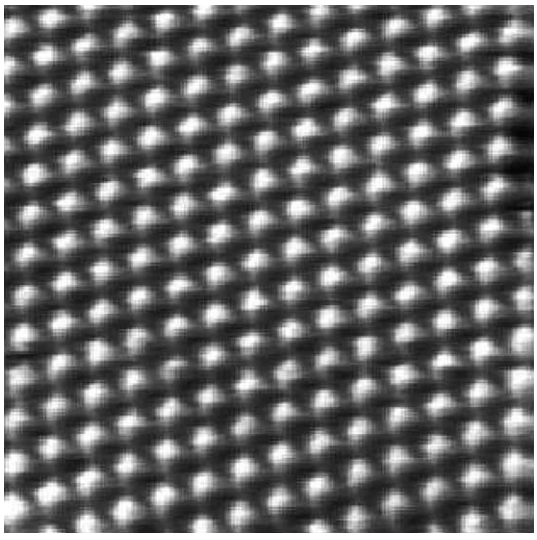

Fig. 3. STM image of the $p(1 \times 1)$ periodicity on the $ErSi_2$ surface for a sample bias voltage of $V_s = -10$ mV, $I_t = 0.4$ nA, size $= 5 \times 5$ nm^2.

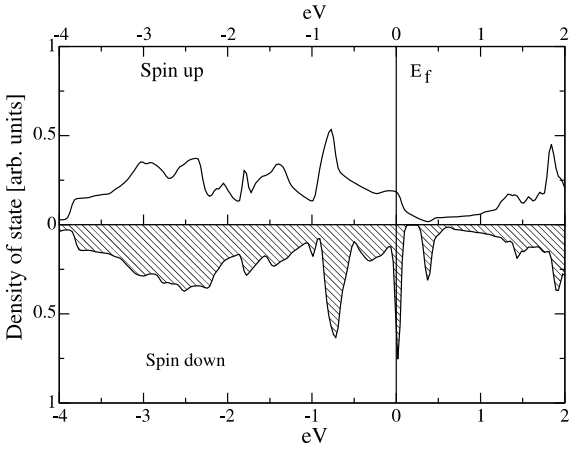

Fig. 4. $ErSi_2$ electronic density of state for Si adatoms. The pz orbital contribution at the density of state is near the Fermi level.

Fig. 5. $ErSi_2$ electronic density of state for Si adatoms. Image simulated with a bias voltage of −10 mV at 2.5 Å of the surface, size = 4.6×4.8 nm^2.

to the tunneling current. Integrals of the electronic density around the different atoms (Fig. 4) show that in the $ErSi_2$ case, electronic structure at the top of the valence band is due to Si pz state. The absence of gap means a semi metallic behavior.

The great spatial extension of the pz orbitals in the $ErSi_2$ structure gives a homogeneous integrated density of state in function of the energy. All the Si atoms of the bilayer have the same electronic structure. We retrieve the same results about the density of state that those already published with the APW method [24]. Some light discrepancies exist with some other works due to differences between the set of parameters and the theoretical method (LMTO + tight binding, Hückel) used during the ab initio calculation [6,20]. The simulated STM images present the same p(1 × 1) periodicity (Fig. 5) for any bias voltages that the experimental STM images.

4.2. The $ErSi_{1.7}$ surface

For Er deposition at coverage over 1 ML, flat 3D islands with hexagonal symmetry are displayed in large scale STM image. The $(\sqrt{3} \times \sqrt{3})R30^\circ$ LEED pattern is found and is explained in the literature by the presence of ordered vacancies in the Si graphite-like planes of the 3D silicide [18]. High-resolution STM images of the filled states reveal a bias voltage dependence as shown in Figs. 6 and 7. Fig. 6 displays an atomic STM image of the filled states for the 3D $ErSi_{1.7}$ silicide surface taken with

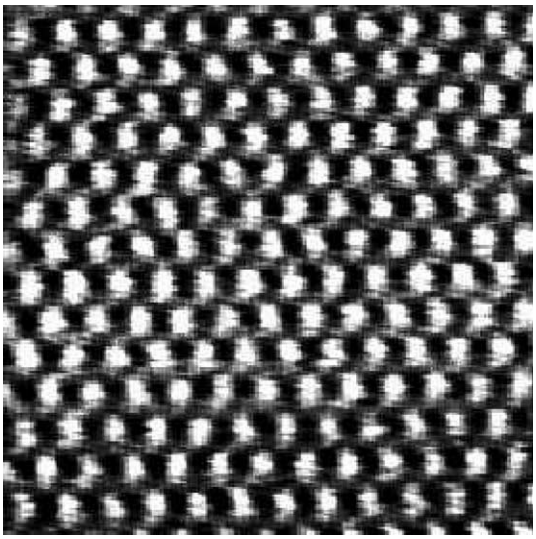

Fig. 6. High-resolution STM image on the 3 D $ErSi_{1.7}$ showing a p(1 × 1) periodicity for a sample bias voltage of $V_s = -37$ mV, $I_t = 2.2$ nA, size = 5×5 nm^2. The LEED pattern corresponding to this surface is a $(\sqrt{3} \times \sqrt{3})R30^\circ$.

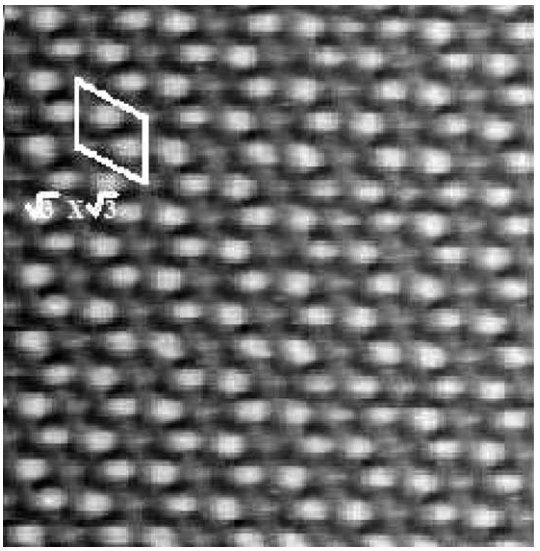

Fig. 7. High-resolution STM image on the 3D $ErSi_{1.7}$ showing a $(\sqrt{3}\times\sqrt{3})R30^\circ$ modulation with a bias voltage of $V_s = -160$ mV, $I_t = 0.4$ nA, size $= 5\times 5$ nm^2. The LEED pattern corresponding to this surface is a $(\sqrt{3}\times\sqrt{3})R30^\circ$.

a bias voltage of $V_s = -37$ mV and tunneling current of $I_t = 2.2$ nA. The image shows a $p(1\times 1)$ reconstruction similar with that presented in Fig. 3 for the 2D silicide.

The measured in-plane periodicity of 3.84 Å, closely corresponds to the $p(1\times 1)$ unit cell of hexagonal Si(1 1 1) or epitaxial $ErSi_2$(0 0 0 1) atomic planes [6,19,20,24]. At lower bias voltage (Fig. 7), an additional $(\sqrt{3}\times\sqrt{3})R30^\circ$ modulation appears clearly on the filled state STM images [4,9,18,21].

The $\sqrt{3}$ modulation is generally quite small but it can be enhanced at particular tunneling conditions as those selected in Fig. 7 ($V_s = -160$ mV, $I_t = 0.4$ nA). Similarity between the STM images of the filled states for the 2D and 3D silicides implies closely related surface terminations. It is apparent from previous works that the states which provide the major contribution to the tunneling current are located near the hole pocket at $\Gamma'(\Gamma)$ for the 3D silicide (2D silicide) in the IBZ (irreducible Brillouin zone) [18]. According to band structure calculations, the electronic states near $\Gamma'(\Gamma)$ have the same physical origin and are due to surface state with Si 3 pz character that are derived from dangling bonds of the layer surface.

In order to simulate the $ErSi_{1.7}$ structure, we have used the same set of parameters in the Wien2k code that for $ErSi_2$. We retrieve some similitude between the two structures. The density of states, as for the $ErSi_2$ structure, is not null at the Fermi level for the silicon atoms in the S1 and S3 sites. We are confronted again at a semi metallic behavior with a modulation of the density of states in function of the energy for the silicon adatoms in S1 and S3 (Figs. 8 and 9). The two

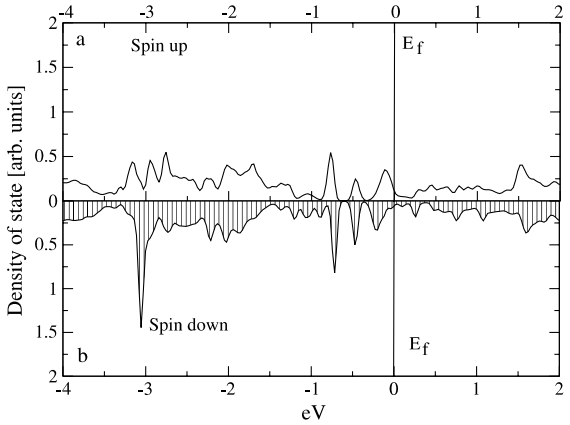

Fig. 8. $ErSi_{1.7}$ electronic density of state for Si adatoms in position S1 (spin up (a) and spin down (b)) above the vacancy.

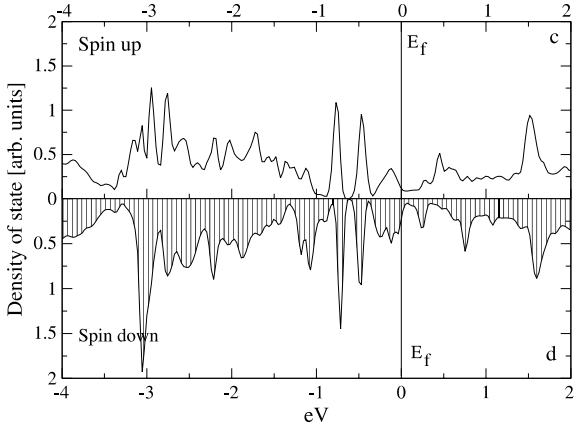

Fig. 9. $ErSi_{1.7}$ electronic density of state for Si adatoms in position S3 (spin up (c) and spin down (d)) at the center of the structure.

surface positions are not equivalent. The sites S3 (Fig. 2) for the silicon atoms on the diagonal of the atomic cell, present a density of state more important that the atoms on sites S1. Our results qualitatively agreed with the results published by Allan et al. on the $ErSi_{1.7}$ DOS. The discrepancies are due to the LMTO plus tight binding method used in their simulation [20]. The peaks are more localized in energy, near the Fermi level between $(E_f + 1.0\,eV)$ and $(E_f - 1.0\,eV)$ due to the pz contribution.

It is admitted that the $ErSi_{1.7}$ surface is terminated by a buckled Si plane with atomic positions very close to the position of the Si atoms on an ideal Si(1 1 1) p(1 × 1) surface. However, two different assumptions have been made in order to explain the STM modulation of the surface in function of the bias voltage. For one group, the $(\sqrt{3} \times \sqrt{3})R30^\circ$ reconstruction is due to a relaxation around 0.2 and 0.3 Å of the upper Si atoms toward either T4 or H3 sites in function of the bias voltage [20,21]. For the second group, the reconstruction $(\sqrt{3} \times \sqrt{3})R30^\circ$ is explained in terms of a small additional buckling of the topmost Si layer because of the underlying vacancy periodicity in the bulk silicide [18]. In this case, the corrugation of the STM images will be due to a spectroscopic effect. Our simulations permit to isolate the different parameters and determine their contribution. In the aim to maintain the optimization of the structure already described, we have chosen to fix the atoms positions [18,21]. The density of states obtained in simulation gives the contribution of the different valence electrons. Using the local integrated density of states, following the Tersoff–Hamann model, we have simulated the constant-current STM topography. The isosurfaces are determined at an average distance of 2.5 Å from the core of the outermost atoms, on a surface of $46 \times 48\ Å^2$ and for different sample bias voltages (+1.0, +0.3, +0.07, −0.07, −0.3, and −1.0 V) (Fig. 10). The bias voltages are taken to permit a comparison with the experimental results already published [18,21].

In comparing the different images in Fig. 10, we can identify an apparent modification of the periodicity in function of the bias voltage. The images simulated at positive voltage (+1.0 V (Fig. 10(a)), +0.3 V (Fig. 10(b))) show a p(1 × 1) lattice modulated by the $(\sqrt{3} \times \sqrt{3})$. The bright spots are separated by 6.7 Å (i.e. $\sqrt{3} \times \sqrt{3}R30^\circ$) as already described experimentally [9,21]. When the bias voltage is diminished (+0.07 V, Fig. 10(c)), we observe only the p(1 × 1) lattice with a distance between spots equal at 3.84 Å. For the bias voltage of −0.3 V, the Si(1 1 1) p(1 × 1) surface is slightly modulated by a $(\sqrt{3} \times \sqrt{3})$. The corrugation disappears again for the others voltages (−0.07, and −1.0 V). This behavior shows that the $(\sqrt{3} \times \sqrt{3})R30^\circ$

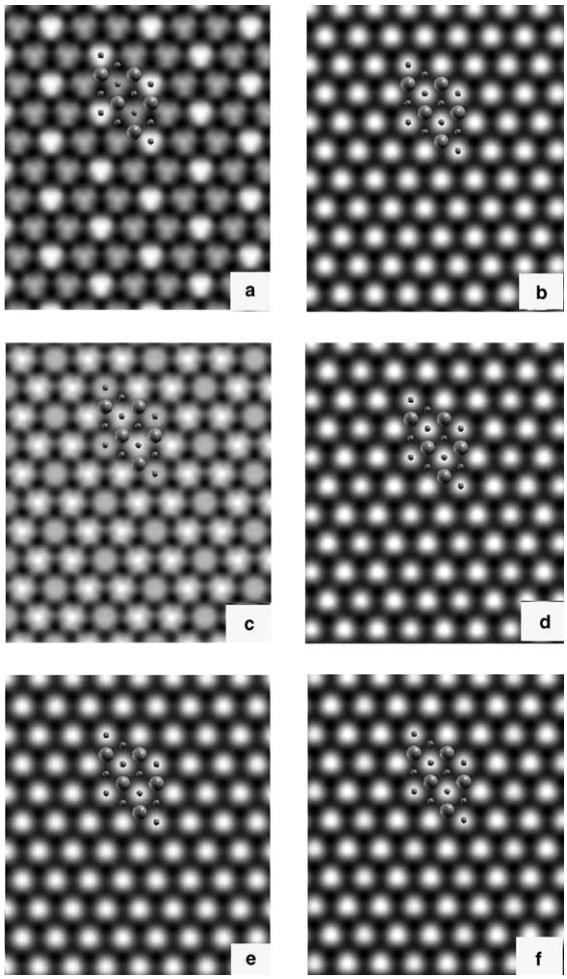

Fig. 10. $ErSi_{1.7}$ electronic density of state for Si adatoms. Image simulated with a sample bias voltage of +1.0 V (a), 0.3 V (b), 0.07 V (c), −0.07 V (d), −0.3 V (e), −1.0 V (f) at 2.5 Å of the surface. The lattice $(\sqrt{3} \times \sqrt{3})R30^\circ$ centered on Si vacancy is superimposed on the images.

periodicity observed in Fig. 10 is due to a real electronic effect of the surface. A relaxation of the upper Si atoms in function of the bias voltage is impossible since in ab initio calculation the position of the different atoms is fixed. The assumption considering the relaxation effect cannot explain the theoretical results. The second group explains the corrugation of the STM image in terms of a small additional buckling of the topmost Si layer because of the underlying vacancy periodicity in bulk silicide. A contour map sketched along the direction $[1\bar{2}1]$ of the $\sqrt{3}\times\sqrt{3}R30^\circ$ reconstruction permits to understand the importance of the vacancy periodicity on the structure (Fig. 11). We observe that under the Si adatoms present on the S1 sites, vacancies are characterized by an absence of density of state. A charge transfer exists between the silicon adatoms of the bilayer and the Er–Si bulk structure. The Er atoms stabilize the $ErSi_{1.7}$ and permit with the vacancies lattice to reduce the number of dangling bonds of the topmost Si layer. We verify the assumption formulated by Magaud et al. [24].

The theoretical results obtained at high positive voltages on the images STM simulated confirm experimental results already obtained (Fig. 10(a) and (b)) [18]. We retrieve the empty states localized on the surface due to the interactions between the Si atoms in the position S1 and the lattice of vacancies. The modulation of the electronic density of state in function of the atoms position and of the energy is induced by the lattice reconstruction. The brutal variation in the density of states produces a modulation of the tunneling current on the theoretical STM images. The intensity of the modulation is bias voltage dependent (Fig. 10). This comportment can be explained by the two geometric nonequivalent sites in surface, one over the vacancy (S1) and the second inside the cell (S3). The maximum in the intensity is provided by the two silicon atoms (site S3) present on the diagonal of the structure cell (Fig. 2) for the negative bias voltages and by the four silicon atoms (site S1) for the high positive bias voltages. In the case of positive bias voltages, it is due to the additional buckling between the Si atoms on the sites S1 and the vacancies. When the bias voltage is diminished, the contribution of occupied states centered on the atom S3 increases, competes with the contribution of the atoms in the positions S1 and corrugates the intensity distribution. This phenomenon is linked to the modulation of the electronic density, which becomes too weak for certain energy [9,21]. It induces the same effect for the theoretical STM images (Fig. 10(c), (d) and (f)).

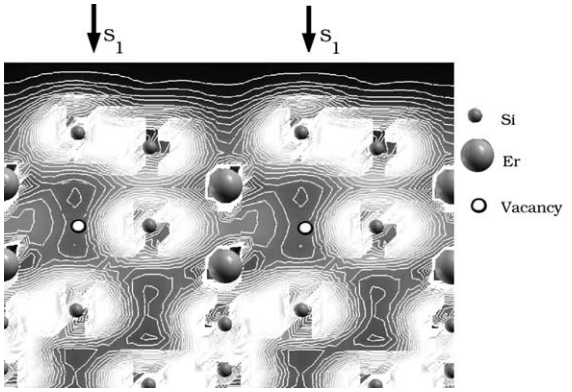

Fig. 11. $ErSi_{1.7}$ contour map of the electronic density of state along the direction $[1\bar{2}1]$. The arrows indicate the Si adatoms on sites S1 (distance between each site 6.7 Å), the black circles correspond to the Si vacancies. A charge transfer exists between the silicon adatoms of the bilayer and the Er–Si bulk structure.

The modulation $\sqrt{3}$ is always present but sometimes masked by the weak variation of the states density as the algorithm treatment shows on the STM simulated images (Fig. 12). This modulation is inferior at 5% of the integrated intensity and depends of the local density of states and of the bias voltage. In order to have a better analysis of the $ErSi_{1.7}$ images simulated in function of the bias voltages, we have modified the contrast of the spot bright for the bias voltages. Usually, the intensity on an image is a linear function of the pixel value. With the use of an exponential function proportional to the pixel value, we can magnify this intensity. An example is shown in Fig. 12. The algorithm treatment on the initial image Fig. 10(d) permits to exhibit the modulation $(\sqrt{3}\times\sqrt{3})$ on the $p(1\times1)$ surface. The obtained data permit to confirm the experimental STM results and the assumption proposed. The corrugation obtained experimentally is related to a spectroscopic effect and not due to a topographic displacement of the atoms.

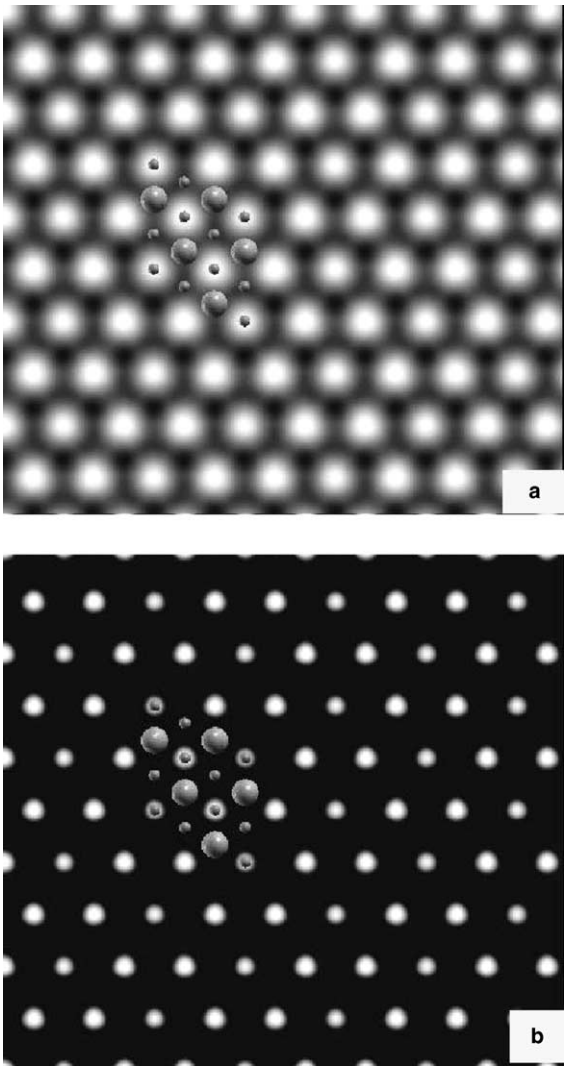

Fig. 12. $ErSi_{1.7}$ electronic density of state for Si adatoms, image simulated (a) and treated (b) with a bias voltage of -0.07 V at 2.5 Å of the surface. The surface lattice $(\sqrt{3}\times\sqrt{3})R30^\circ$ centered on Si vacancies is represented by its atoms.

5. Conclusion

The surface structure of the $ErSi_{(2-x)}$ compounds has been investigated by combining STM results and theoretical simulations. We retrieve with the LAPW method some results already published. However, with the progress in the ab initio simulation, its became possible to reconstruct high-resolution STM images. The density of states, calculated and integrated near the Fermi level, permits to show a strong dependence of the observed $(\sqrt{3}\times\sqrt{3})R30^\circ$ modulation with the bias voltage. For the 2D and 3D erbium silicide, a Si buckled layer terminates the surface. For the 3D erbium silicide, the small modulation with the periodicity $(\sqrt{3}\times\sqrt{3})R30^\circ$ induced by the vacancies is observed and explained in function of the spectroscopic voltage and not in function of the atoms displacements.

Acknowledgments

The authors wish to thank Dr. Koitzsch of the Institute of Physic, University of Neufchâtel, for the help on the AlB_2 structure of the erbium disilicide.

References

[1] M.H. Tuilier, C. Pirri, D. Berling, D. Bolmont, G. Gewinner, P. Wetzel, Surf. Sci. 555 (2004) 94.
[2] J. Yang, Q. Cai, X.D. Wang, R. Koch, Surf. Sci. 526 (2003) 291.
[3] P. Wetzel, T. Angot, C. Pirri, G. Gewinner, Surf. Sci. 383 (1997) 340.
[4] T. Roge, F. Palmino, C. Savall, J.C. Labrune, C. Pirri, Surf. Sci. 383 (1997) 350.
[5] S. Saintenoy, P. Wetzel, C. Pirri, D. Bolmont, G. Gewinner, Surf. Sci. 331–333 (1995) 546.
[6] L. Stauffer, A. Mharchi, C. Pirri, P. Wetzel, D. Bolmont, G. Gewinner, C. Minot, Phys. Rev. B 47 (1993) 10555.
[7] M. Lohmeier, W. Huisman, E. Vlieg, A. Nishiyama, C.I. Nicklin, T. Turner, Surf. Sci. 345 (1996) 247.
[8] M. Unewisse, J. Storey, J. Appl. Phys. 72 (1992) 2367.
[9] J.A.M. Gago, J.M.G. Rodriguez, J.Y. Veuillen, Surf. Sci. 366 (1996) 491.
[10] A. Irrera, D. Pacifici, M. Miritello, G. Franzo, F. Priolo, F. Iacona, D. Sanfilippo, G.D. Stefano, P. Fallica, J. Physica E 16 (2003) 395.
[11] A. Polman, B. Min, J. Kalkman, T.J. Kippenberg, K.J. Vahala, Appl. Phys. Lett. 84 (2004) 1037.
[12] A. Kenyon, C. Chryssou, C. Pitt, T.S. Iwayama, D. Hole, N. Sharma, C. Humphreys, Mater. Sci. Eng. B 81 (2001) 19.
[13] M.J.A. de Dood, A. Polman, J.G. Fleming, Phys. Rev. B. 67 (2003) 115106.
[14] G. Kik, M.L. Brongersma, A. Polman, Appl. Phys. Lett. 76 (2000) 2325.
[15] A.J. Kenyon, C.E. Chryssou, C.W. Pitt, T. Shimizu-Iwayama, D.E. Hole, N. Sharma, C.J. Humphreys, J. Appl. Phys. 91 (2002) 367.

[16] K. Watanabe, M. Fujii, S. Hayashi, J. Appl. Phys. 90 (2001) 4761.
[17] S. Auffret, J. Pierre, B. Lambert, J. Soubeyroux, J.A. Chroboczek, Physica B 162 (1990) 271.
[18] P. Wetzel, S. Saintenoy, C. Pirri, D. Bolmont, G. Gewinner, T. Roge, F. Palmino, C. Savall, J.C. Labrune, Surf. Sci. 355 (1996) 13.
[19] M.H. Tuilier, P. Wetzel, C. Pirri, D. Bolmont, G. Gewinner, Phys. Rev. B 50 (1994) 2333.
[20] G. Allan, I. Lefebvre, N.E. Christensen, Phys. Rev. B 48 (1993) 8572.
[21] J.A. Martin-Gago, J.M. Gomez-Rodriguez, J.Y. Veuillen, Phys. Rev. B 55 (1997) 5136.
[22] P. Blaha, K. Schwarz, G.K.H. Madsen, D. Kvasnicka, J. Luitz (Eds.), Computer code WIEN2k, An Augmented Plane Wave Plus Local Orbitals Program for Calculating Crystal Properties, Austria, Vienna Karlheinz Schwarz Technical Universität, 2001.
[23] J. Tersoff, D.R. Hamann, Phys. Rev. B 31 (1985) 805.
[24] L. Magaud, J.Y. Veuillen, D. Lollman, T.A. NguyenTan, D.A. Papaconstantopoulos, M.J. Mehl, Phys. Rev. B 46 (1992) 1299.